

Strength prediction of rotary brace damper using MLR and MARS

I. Mansouri¹, M. Safa^{*2}, Z. Ibrahim², O. Kisi³, M.M. Tahir⁴, S. Baharom⁵ and M. Azimi⁶

¹Department of Civil Engineering, Birjand University of Technology, Birjand, Iran

²Department of Civil Engineering, University of Malaya, Kuala Lumpur, Malaysia

³Center for Interdisciplinary Research, International Black Sea University, Tbilisi, Georgia

⁴UTM CRC, Institute for Smart Infrastructure and Innovative Construction, UTM, Johor Bahru, Malaysia

⁵Department of Civil and Structural Engineering, National University of Malaysia, Malaysia

⁶Department of Quantity Surveying, Universiti Teknologi Malaysia, Johor Bahru, Malaysia

(Received October 25, 2015, Revised July 12, 2016, Accepted September 6, 2016)

Abstract. This study predicts the strength of rotary brace damper by analyzing a new set of probabilistic models using the usual method of multiple linear regressions (MLR) and advanced machine-learning methods of multivariate adaptive regression splines (MARS). Rotary brace damper can be easily assembled with high energy-dissipation capability. To investigate the behavior of this damper in structures, a steel frame is modeled with this device subjected to monotonic and cyclic loading. Several response parameters are considered, and the performance of damper in reducing each response is evaluated. MLR and MARS methods were used to predict the strength of this damper. Displacement was determined to be the most effective parameter of damper strength, whereas the thickness did not exhibit any effect. Adding thickness parameter as inputs to MARS and MLR models did not increase the accuracies of the models in predicting the strength of this damper. The MARS model with a root mean square error (RMSE) of 0.127 and mean absolute error (MAE) of 0.090 performed better than the MLR model with an RMSE of 0.221 and MAE of 0.181.

Keywords: rotary brace damper; passive energy dissipation; nonlinear response; MLR; MARS; damper strength

1. Introduction

1.1 General

In the past decades, considerable research and development have been conducted and achieved in constructing safer and robust civil structures by applying energy-dissipating systems (Symans, Charney *et al.* 2008), which adopt different energy-dissipating devices, such as shear connectors (Shariati, Ramli Sulong *et al.* 2010, Shariati, Ramli Sulong *et al.* 2011, Shariati, Ramli Sulong *et al.* 2011, Shariati, Ramli Sulong *et al.* 2012, Ataei, Bradford *et al.* 2015) or dampers (Daie, Jalali

*Corresponding author, Research Assistant, E-mail: maryamsafa1991@gmail.com

et al. 2011, Faris, Khalid *et al.* 2012, Jalali, Daie *et al.* 2012). In few cases, also they use advance concrete technology (Muhammad, Keyvanfar *et al.* 2015, Muhammad, Shafaghat *et al.* 2016) which is not in scope of this study. The structure in this technique is equipped with designated energy dissipating devices (EDD) in which a portion of energy that originates from ground vibrations is deflected. Dampers, which utilize metallic yielding for energy dissipation, are used extensively because these devices are more economical, insensitive to vibration frequency, and require minimal compared with other types of EDDs.

Dampers are classified as shape memory alloys (SMA) and mass dampers based on their friction performance, metal (flowing), viscosity, and viscoelasticity. Dampers exhibit high energy absorbance, can be easily installed and replaced, and coordinate with other structure members (Heysami 2015).

Moment-resisting frames, braced frames, and shear walls are examples of conventional lateral force-resisting structural systems used in seismic design. Other alternatives for resisting lateral loads have been successfully proposed in recent years, which include eccentric-braced frame and K-braced frame (Scholl 1984). Brace damper is another engineered alternative (Scholl 1984). Selecting a proper structure system to provide lateral force resistance is one of the most difficult tasks for structural engineers. Braced steel frames effectively provide lateral stiffness and strength.

However, conventional concentric braced steel frames are brittle and do not result in lateral deformation. Properly designed ductile moment-resisting space frames provide adequate resistance to earthquake energy demands but result in excessive drifts, which in turn causes structural and non-structural damage during severe earthquakes, and require high quantities of construction steel. Integrating these two approaches to provide resistance to lateral forces would produce economical structures and effectively perform under lateral force loading conditions, such as earthquakes (Abdulrahman, Ismail *et al.* 2011, Imaduddin, Mazlan *et al.* 2013).

Rotary dampers are simple dampening mechanisms, which can be incorporated to structural design and used in braced systems. Passive vibration isolation utilizes materials and mechanical linkages (Muhammad and Ismail 2012, Muhammad, Ismail *et al.* 2012, Hafizah, Bhutta *et al.* 2014). The types of rotary dampers and available literature on the behavior of these dampers are numerous. Pranoto and Nagaya (Pranoto and Nagaya 2005) developed 2DOF-type and rotary-type shock absorber dampers by using MRF and the efficiencies of these dampers. Waleed *et al.* (Faris, Khalid *et al.* 2012) investigated the efficiency of a rotor-bearing system that contains composite and non-composite squeeze film dampers. A heavy off-road wheeled vehicle with a semi-active rotary damper was examined by Elsa and Holmanb (1999). A shear-mode rotary magnetorheological damper was proposed by Tse and Chang for small-scale structural control experiments. Other proposed rotary dampers include rotary oil damper by Umemura (1994) and rotary damper with improved connection between cap and housing by Kawamoto *et al.* (Kawamoto, Yamaguchi *et al.* 1993). A novel rotary damping mechanism was developed by Burgess and Clarkson for aerospace deployment systems. Imaduddina *et al.* studied the design and modeling review of a rotary magnetorheological damper. Noresson *et al.* (Noresson, Ohlson *et al.* 2002) designed a electrorheological damper by using finite element analysis. Yazid *et al.* (Yazid, Mazlan *et al.* 2014) created a magnetorheological damper, which combines shear and squeeze modes.

Rotary brace damper (RBD), which is an innovative supplemental lateral-load-resisting system suitable for discrete rehabilitation action, is proposed. The system is easily connected to existing frames through conventional construction techniques, such as high-strength bolts, turnbuckles, and pad eyes.

For seismic applications, an appropriate displacement-based device must generally exhibit (1) elastic stiffness that can adequately withstand in-service lateral loads, such as wind; (2) the yield strength of a damper, which exceeds anticipated in-service lateral loads, such that the device is activated only in an earthquake event; (3) high-energy dissipative capability; and (4) stable hysteretic force-displacement response, which can be modeled numerically (Azimi, Adnan *et al.* 2014, Chan and Wong 2014, Azimi, Adnan *et al.* 2015, Faridmehr, Osman *et al.* 2015). This damper is believed to fulfill the criteria stated above.

The strength prediction of this damper is important in investigating its behavior. Many researchers used the soft computing or statistical method for modelling (Schumacher and Shariati 2013, Moghaddam, Soltani *et al.* 2015, Shariati and Schumacher 2015, Shariati, Schumacher *et al.* 2015, Soltani, Moghaddam *et al.* 2015, Moghaddam, Soltani *et al.* 2016). Hence, soft computing methods are employed after a structural analysis of the damper is conducted.

Multiple linear regressions method (MLR) is a method that enables additional factors to be included individually in the analysis to estimate the effects of these factors. The MLR is a useful method to measure the effect of various and simultaneous factors on a single dependent parameter. Simple regression omits parameter bias. Thus, multiple regressions are often vital even when the effect of only one of the independent parameters is analyzed.

Multivariate adaptive regression splines (MARS) is a nonlinear and non-parametric regression method (Friedman 1991). The greatest advantage of MARS is its ability to explore the intricate nonlinear relations between a response parameter and predictor parameters. MARS can identify input parameters that significantly affect responses. MLR and MARS effectively handle prediction problems and have been successfully employed in civil engineering (Mohammadhassani, Nezamabadi-Pour *et al.* 2013, Mohammadhassani, Nezamabadi-Pour *et al.* 2013, Samui and Kim 2013, Zhang and Goh 2013, Huang, Sheen *et al.* 2014, Mohammadhassani, Suhatriil *et al.* 2014, Silva, Neves *et al.* 2014, Huang, Xu *et al.* 2015, Mansouri and Kisi 2015, McGann, Bradley *et al.* 2015, Salazar, Toledo *et al.* 2015). A novel collection of the probabilistic strength of RBD models is proposed in the current study, which uses conventional MLR method and advanced machine-learning methods of MARS to investigate the parameters that affect the strength of RRRB dampers.

1.2 Damper description

Fig. 1 shows the rotary brace damper. The parts are joined together using adopting joining methods.

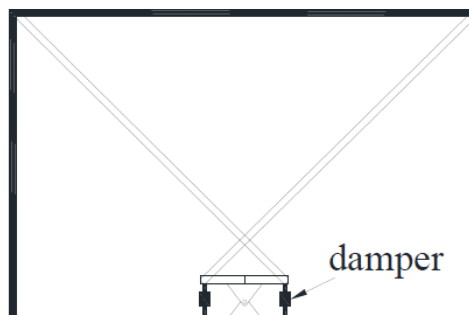


Fig. 1 Rotary brace damper (Kang and Tagawa 2013)

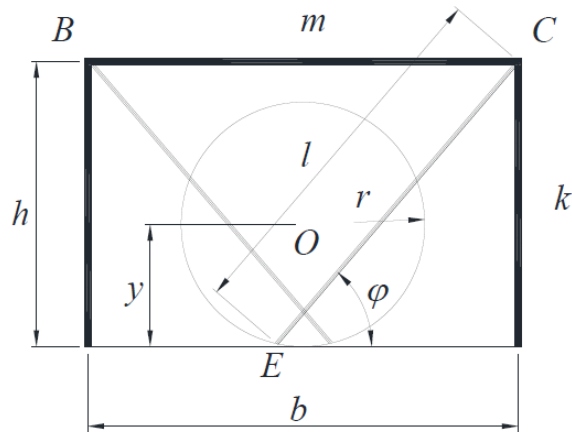


Fig. 2 Different damper conditions (Chan and Wong 2014)

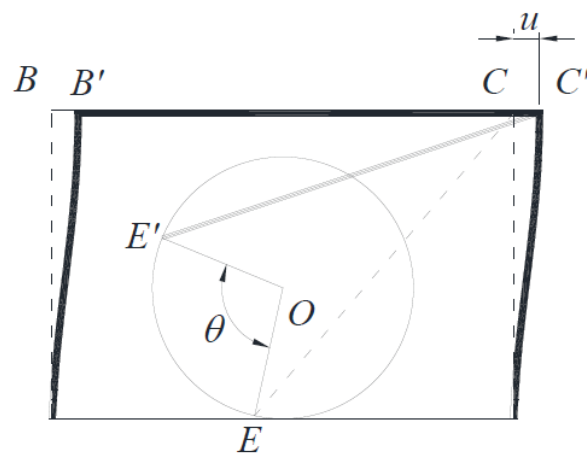


Fig. 3 Rotary brace damper with deformed shape

1.3 Basic concepts of the damper

The damper is built according to the concept of rotational friction and sliding (Fig. 2), when the frame is dislocated in the loading path, the damper rotate and slide along with the bracings, thereby allowing the bracings to move and pull and push to mitigate the base motion.

1.4 Basic concept of damper in frame structure

Various approaches have been adopted to install the damper to a frame structure. For instance, the damper could be installed with two diagonal bracings and two dampers, as shown in Fig. 3. When a frame structure is stimulated with a large force by a lateral external force, the top of the structure displaces horizontally as a result of this force. This horizontal motion will be resisted by the braced system. When the bracing is moved, it is subjected to compression and the damper dissipates energy. During an earthquake, the structural frame of a building, as shown in Fig. 3, will

be propelled from left to right repeatedly. Hence, energy is dissipated because the bracings are subjected to tension and compression. As depicted, the damper has simple components, thereby allowing ease of assembly and flexibility of arrangement.

2. Methods

2.1 Structural analysis

The expansion of a precise analytical finite element (FE) model for the rotary brace damper has been used. The finite element method is a numerical technique employed to identify approximate solutions to boundary value problems for partial differential equations (Sinaei, Shariati *et al.* 2012, Azimi, Ponraj *et al.* 2015, Khorramian, Maleki *et al.* 2015, Shariati, Ramli Sulong *et al.* 2015, Alhajri, Tahir *et al.* 2016, Tahmasbi, Maleki *et al.* 2016). The general-purpose FE analysis program ABAQUS (Hibbitt, Karlsson *et al.* 1988) is used for this purpose. The material and geometric nonlinearities are both considered in the FE models using the standard material properties. The results of the primary finite element analysis were used to conduct soft computing analysis of this damper.

2.2 Multivariate Adaptive Regression Splines (MARS)

Friedman (1991) initially introduced MARS as a pliable method to organize relations, which are almost augmentative or interact with a few parameters. When data are sparse, MARS does not produce assumptions on the basic functional relation between dependent and independent parameters to assess the general functions of high-dimensional arguments (Friedman 1991, Samui and Kim 2013). MARS could estimate the contribution of the basis functions to allow the interactive and additive effects of predictors to specify a response parameter. To establish MARS, a base function (term) is fitted to preferable independent parameter intervals. Splines (sometimes referred to as piece-wise polynomials) generally consist of parts smoothly coupled together. The points of interface between parts are referred to as knots, which are indicated as t . Two-sided truncated power functions are used as spline basis functions, as characterized in Eqs. (1) and (2). An illustration is provided in Fig. 4 ($q=1$; $t=0.5$)

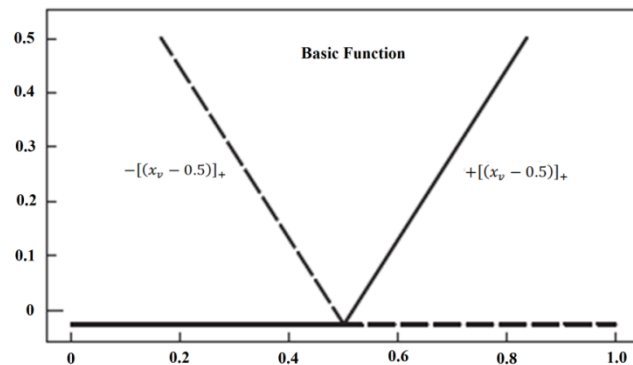


Fig. 4 Basis function

$$[-(x_v - t)]_+^q = \begin{cases} (t - x_v)^q & \text{if } x_v < t \\ 0 & \text{otherwise} \end{cases} \quad (1)$$

$$[+(x_v - t)]_+^q = \begin{cases} (t - x_v)^q & \text{if } x_v \geq t \\ 0 & \text{otherwise} \end{cases} \quad (2)$$

where ($q \geq 0$) is the power to which splines are raised and specifies the degree of smoothness of the consequent function estimate; $q=1$ is used in the current investigation; and $[\]_+$ ensures that positive values are obtained.

Interaction basis functions are produced by multiplying an available term with a truncated linear function, which involves a novel parameter. In this case, the MARS model is established by using both the available term and the generated interaction base function. Restrictions in searching for new basis functions may occur when a maximum user order is set. Eqs. (3) and (4) represent the formulas for the interaction basis function and general MARS function, respectively.

$$B_m(x) = \prod_{j=1}^{k_m} [s_{mj} \times (x_{v(m,j)} - t_{(m,j)})]_+, \quad (3)$$

$$\hat{y} = \hat{f}_M(x) = c_0 + \sum_{m=1}^M c_m B_m(x), \quad (4)$$

where K_m denotes the number of truncated linear functions multiplied in the m th basis function. K_m must not be larger than the maximum interaction in parameter I_{\max} . Hence, before recreating the MARS model, I_{\max} must first be specified. $x_{v(m,j)}$ is the input parameter that corresponds to the j th truncated linear function in the m th term; $t_{m,j}$ is the node value that corresponds to parameter $x_{v(m,j)}$; $s_{m,j}$ is the selected sign +1 or -1; \hat{y} is the dependent parameter, which is estimated by the MARS model; c_0 is a constant; $B_m(x)$ is the m th base function, which may be a single spline base function; and c_m is the factor of the m th basis function.

A two-stage process, which includes forward and backward phases, was used to construct the final MARS model. The forward stage was initiated with the base function $h_0(x)=1$. Nodes were selected spontaneously. To define a pair of basis functions, candidate nodes were placed within the range of each predictor parameter at random positions. The node and its corresponding pair of base functions are adopted at each stage by the model to significantly decrease the sum-of-squares residual error. The basis functions are added continuously until the maximum number of basis functions M_{\max} is achieved, (Friedman 1991). M_{\max} is set by a user as referenced in Friedman (1991) (Friedman 1991). The forward phase selection of the basis function results in a substantially complex and over-fitted model. Despite the poor predictive capabilities for a new database (testing data), the model fits well with the training data.

2.3 Multiple linear regression

MLR analysis, which is a deployment of the simple linear regression method, is utilized for the purpose of providing mathematical relation between a dependent output parameter and several independent expository parameters. The MLR is among the most commonly applied statistical approaches, particularly for the analysis of experiments where predictor parameters are controlled by the experimenter. The basic assumption in MLR, as in simple linear regression, is that the error term is usually spread with zero mean and unknown variance, independent of the expository parameters. Hence, the scatterplots of the residuals need to be examined against both the fitted parameters and the independent parameter to determine the suitability of an MLR model. MLR model is considered to be appropriate when no systematic pattern is exhibited by the scatterplots. A normal probability plot also needs to be constructed to investigate the normality of the

distribution of the residuals. The points in the plot will nearly pursue a straight line if the distribution is normal.

The MLR is usually applied in a stepwise manner in which until a satisfactory model is achieved, the independent parameters are added to the model consecutively according to their importance. Hence, the key purpose of this regression method is to determine the important independent parameters among candidate parameters that impress a dependent parameter using analysis of variance (ANOVA). In ANOVA, the F statistic test asserts that no important relation exist between independent parameters and a dependent parameter (null hypothesis), whereas the t statistic test states that no relationship exists between an individual independent parameter and a dependent parameter (null hypothesis). The null hypothesis is refused should a p value be less than a particular importance level. For the F statistic, a p value less than the significant level indicates that at least one of the parameters in the model is important, while for the t statistic, a p value less than the prescribed importance level indicates that the evaluated independent parameter is important. Therefore, linear regressions are carried out in a stepwise manner until the model achieves the condition where the p value for all predictor parameters in the t statistic is less than the significant level. A reasonable importance level is conventionally 0.05 or less.

3. Results and application

In the investigation, rotary damper strength was modelled by applying the MARS and MLR models. Several parameters were selected as inputs for the applied models. Four different input compositions were used based on correlation analysis; the cross-validation procedure was applied for each model by apportioning the data into three subsets. The statistical parameters of the damper strength data were given for each set in Table 1. Datasets used in training and testing of each model are also provided in Table 2. Table 2 clearly shows that each dataset has various ranges, and D3 has higher Sx than the other datasets.

In Table 2, M1 is model 1 and so on. A comparison between the MARS and MLR models was conducted in relation to root mean square errors (RMSE), mean absolute errors (MAE), and determination coefficient (R^2) indexes. The RMSE and MAE are given as

Table 1 The statistical parameters of strength damper data set (units mm)

Data set	x_{mean}	Sx	Csx	x_{min}	x_{max}
D1	1.124	0.601	-0.494	10^{-14}	2.453
D2	1.145	0.578	-0.334	10^{-14}	2.356
D3	1.145	0.623	-0.216	10^{-14}	2.636

x_{mean} , Sx , Csx , x_{min} and x_{max} indicate the overall mean, standard deviation, skewness, minimum and maximum, respectively.

Table 2 Data sets used for training and testing

Cross validation	Trainin data set	Test data set
M1	D1+D2	D3
M2	D1+D3	D2
M3	D2+D3	D1

Table 3 Comparison of the MARS and MLR models-Displacement input

Statistics	Cross validation	Test data set	Method	
			MARS	MLR
RMSE	M1	D3	0.257	0.321
	M2	D2	0.227	0.335
	M3	D1	0.216	0.328
	Mean		0.233	0.328
MAE	M1	D3	0.171	0.251
	M2	D2	0.150	0.263
	M3	D1	0.150	0.258
	Mean		0.157	0.257
R	M1	D3	0.830	0.783
	M2	D2	0.845	0.741
	M3	D1	0.871	0.767
	Mean		0.849	0.764

$$RMSE = \sqrt{\frac{1}{N} \sum_{i=1}^N (Strength_{i,o} - Strength_{i,e})^2} \quad (5)$$

$$MAE = \frac{1}{N} \sum_{i=1}^N |Strength_{i,o} - Strength_{i,e}|, \quad (6)$$

where N represents the number of data, $Strength_{i,o}$ is the observed damper strength values, and $Strength_{i,e}$ is the estimate of the model.

Table 3 presents the test results of the MARS and MLR models for input composition (1),

The average efficiencies of the models showed that the MARS models are more accurate than the MLR models in terms of estimating damper strength. The foremost results were generally

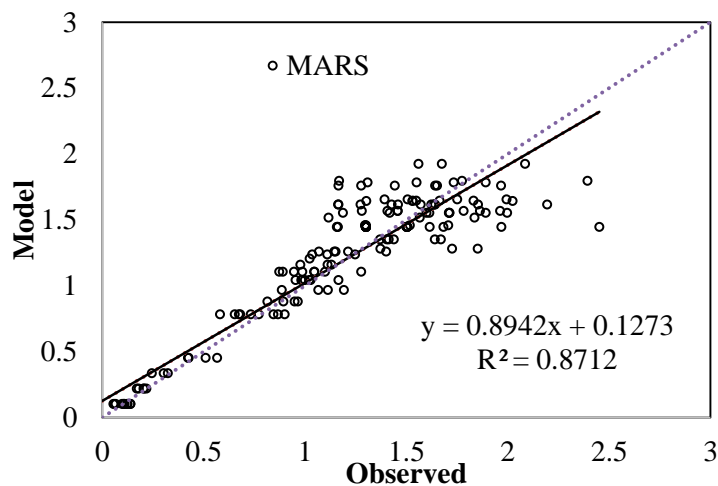


Fig. 5 Observed and estimated forces by the MARS and MLR models with displacement input-M3 dataset

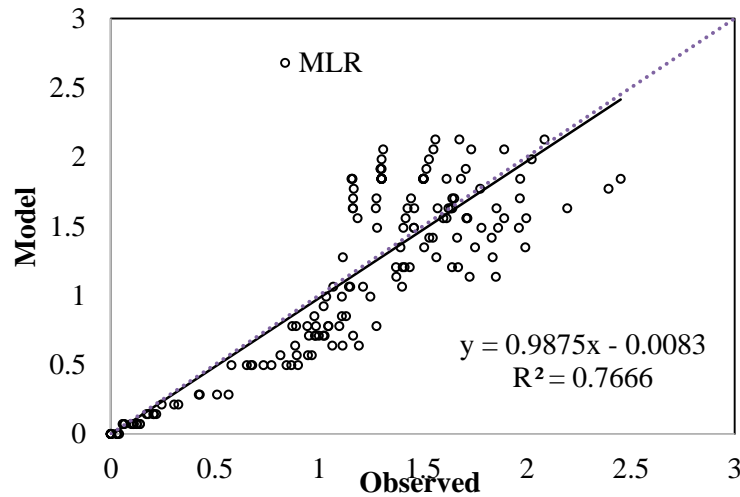


Fig. 5 Continued

Table 4 Comparison of the MARS and MLR models-Displacement and damper thickness inputs

Statistics	Cross validation	Test data set	Method	
			MARS	MLR
RMSE	M1	D3	0.226	0.311
	M2	D2	0.206	0.314
	M3	D1	0.200	0.307
		Mean	0.211	0.311
MAE	M1	D3	0.162	0.240
	M2	D2	0.132	0.242
	M3	D1	0.144	0.246
		Mean	0.146	0.243
R	M1	D3	0.868	0.756
	M2	D2	0.873	0.722
	M3	D1	0.890	0.753
		Mean	0.877	0.744

captured from the M3 model (D1 test dataset), while the M1 model (D3 test dataset) provided the worst results. The major cause for these results may be because the data range of the D3 test dataset exceeded those of the other test data (D1 and D2) limits (see Table 2), The maximum value ($x_{\max}=2.636$) of the D3 test database is higher than those of the other test databases. Training with D1 and D2 datasets cause extrapolation problems for the models used in estimating high damper strength values. Standard deviation is also higher for the D3 test database than those of the others. The MARS model increased the RMSE and MAE accuracies of the MLR model by 41% and 64%, respectively. Damper strength assessments of the applied models are illustrated in Fig. 5 for the M3 models. The figures evidently show that the MARS model has less scattered assessments than the MLR model.

The test results of the MARS and MLR models in measuring damper strength are given in Table 4 for input combination (2).

Similar to the former application, the MARS models performed better than the MLR models. In this case, the best results were also obtained through the M3 model but the M3 models also provided the worst precision. The MARS model enhanced the RMSE and MAE accuracies of the MLR model by 47% and 66%, respectively. Fig. 6 demonstrates the scatterplots of the applied models in measuring damper strength for the M3 models.

The figures clearly show that the estimations of the MARS model are near the corresponding observed damper strength values than the MLR model. Comparison of Tables 5 and 6 indicates that adding damper thickness input increases the models' accuracies. The RMSE of the MARS and MLR models were reduced by 10% and 6%, respectively.

Table 5 compares the test results of MARS and MLR models in measuring damper strength for input composition (3).

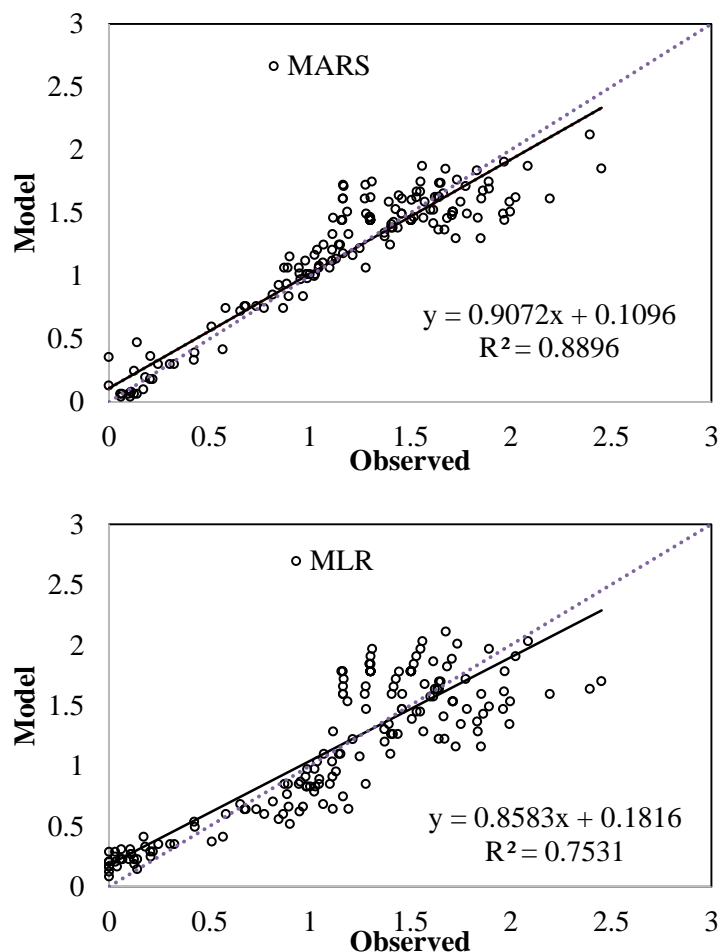


Fig. 6 Observed and estimated forces by the MARS and MLR models with displacement and damper thickness inputs-M3 dataset

Table 5 Comparison of the MARS and MLR models-Displacement, damper thickness and diameter inputs

Statistics	Cross validation	Test data set	Method	
			MARS	MLR
RMSE	M1	D3	0.142	0.215
	M2	D2	0.120	0.219
	M3	D1	0.120	0.228
	Mean		0.127	0.221
MAE	M1	D3	0.099	0.165
	M2	D2	0.083	0.186
	M3	D1	0.087	0.191
	Mean		0.090	0.181
R	M1	D3	0.948	0.882
	M2	D2	0.957	0.860
	M3	D1	0.961	0.859
	Mean		0.955	0.867

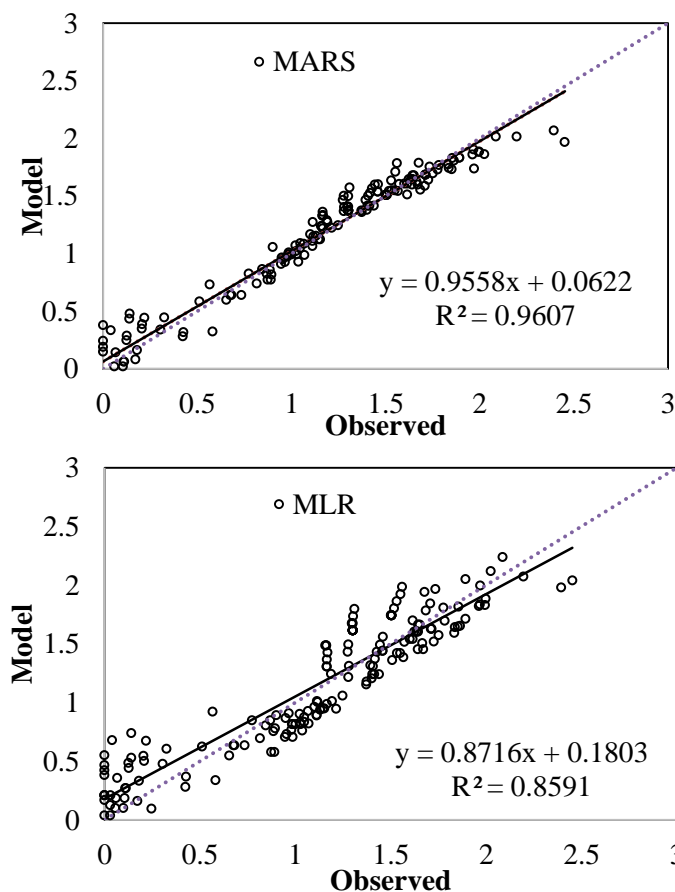


Fig. 7 Observed and estimated forces by the MARS and MLR models with displacement, damper thickness, and diameter inputs-M3 dataset

Table 6 Comparison of the MARS and MLR models-displacement, damper thickness, diameter, and plate thickness inputs

Statistics	Cross validation	Test data set	Method	
			MARS	MLR
RMSE	M1	D3	0.142	0.215
	M2	D2	0.120	0.219
	M3	D1	0.120	0.228
	Mean		0.127	0.221
MAE	M1	D3	0.099	0.166
	M2	D2	0.083	0.187
	M3	D1	0.087	0.192
	Mean		0.090	0.182
R	M1	D3	0.948	0.881
	M2	D2	0.957	0.859
	M3	D1	0.961	0.859
	Mean		0.955	0.866

The MARS models provide better assessments than the MLR models based on the above table. The MARS model enhanced the RMSE and MAE accuracies of the MLR model by 74% and 101%, respectively. The damper strength estimates are shown in Fig. 7.

The MARS model obviously provided better estimates compared to the MLR model as shown in the figure. An analogy of the average accuracies in Tables 4 and 5 reveals that adding diameter input to the models considerably increases precision in estimating damper strength. The RMSE of the MARS and MLR models were reduced by 66% and 41%, respectively. The model results in the test period are reported in Tables 6 for input composition (4),

The results are similar to those of previous applications. The damper strength assessments of each model are illustrated in Fig. 8.

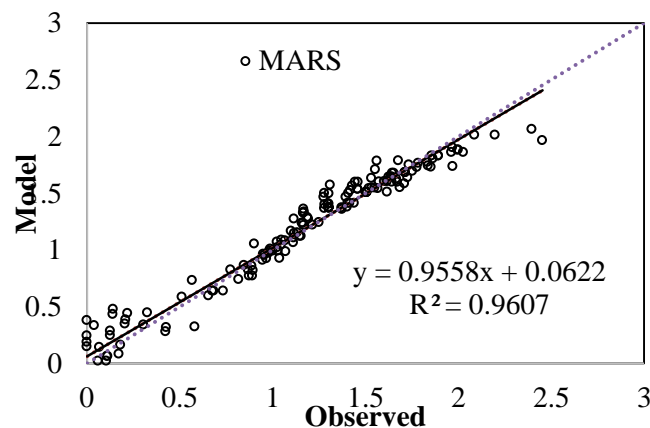


Fig. 8 Observed and estimated forces by the MARS and MLR models with displacement, diameter, and plate thickness inputs-M3 dataset

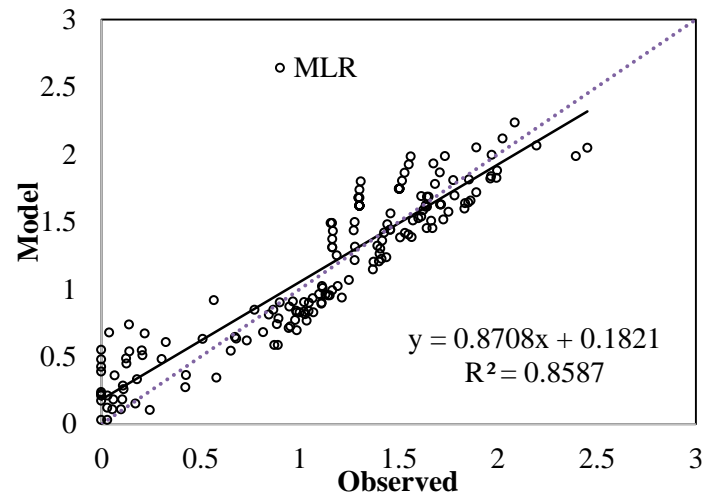


Fig. 8 Continued

Adding plate thickness input to the MARS and MLR models does not increase model accuracy, indicating that parameter is not effective on damper strength. The regression tree of the optimal MARS model for the D1 test dataset is given in Table 7.

Table 7 Regression tree obtained from MARS in estimating damper strength for the D1 test dataset

```

if (x3 <= 0.00018) then f1_1 = 0
  if (0.00018 < x3 < 0.00032) then begin
    p1_1 = (2*(0.00032) + (0.00018) - 3*(0.00025)) / ((0.00032) - (0.00018))^2
    r1_1 = (2*(0.00025) - (0.00032) - (0.00018)) / ((0.00032) - (0.00018))^3
    f1_1 = p1_1*(x3-(0.00018))^2 + r1_1*(x3-(0.00018))^3
  end
  if (x3 >= (0.00032)) then f1_1 = x3 - (0.00025)
  BF1 = f1_1
  if (x3 <= 0.00018) then f2_1 = -(x3 - (0.00025))
  if (0.00018 < x3 < 0.00032) then begin
    p2_1 = (3*(0.00025) - 2*(0.00018) - (0.00032)) / ((0.00018) - (0.00032))^2
    r2_1 = ((0.00018) + (0.00032) - 2*(0.00025)) / ((0.00018) - (0.00032))^3
    f2_1 = p2_1*(x3-(0.00032))^2 + r2_1*(x3-(0.00032))^3
  end
  if (x3 >= (0.00032)) then f2_1 = 0
  BF2 = f2_1
  if (x2 <= 3e-005) then f3_1 = 0
  if (3e-005 < x2 < 5.5e-005) then begin
    p3_1 = (2*(5.5e-005) + (3e-005) - 3*(4e-005)) / ((5.5e-005) - (3e-005))^2
    r3_1 = (2*(4e-005) - (5.5e-005) - (3e-005)) / ((5.5e-005) - (3e-005))^3
    f3_1 = p3_1*(x2-(3e-005))^2 + r3_1*(x2-(3e-005))^3
  end
  if (x2 >= (5.5e-005)) then f3_1 = x2 - (4e-005)
  BF3 = f3_1

```

Table 7 Continued

```

if (x2 <= 3e-005) then f4_1 = -(x2 - (4e-005))
  if (3e-005 < x2 < 5.5e-005) then begin
p4_1 = (3*(4e-005) - 2*(3e-005) - (5.5e-005)) / ((3e-005) - (5.5e-005))^2
r4_1 = ((3e-005) + (5.5e-005) - 2*(4e-005)) / ((3e-005) - (5.5e-005))^3
f4_1 = p4_1*(x2-(5.5e-005))^2 + r4_1*(x2-(5.5e-005))^3
  end
  if (x2 >= (5.5e-005)) then f4_1 = 0
    BF4 = f4_1
    if (x1 <= 1.5e-005) then f5_1 = 0
      if (1.5e-005 < x1 < 2.2e-005) then begin
p5_1 = (2*(2.2e-005) + (1.5e-005) - 3*(1.9e-005)) / ((2.2e-005) - (1.5e-005))^2
r5_1 = (2*(1.9e-005) - (2.2e-005) - (1.5e-005)) / ((2.2e-005) - (1.5e-005))^3
f5_1 = p5_1*(x1-(1.5e-005))^2 + r5_1*(x1-(1.5e-005))^3
      end
      if (x1 >= (2.2e-005)) then f5_1 = x1 - (1.9e-005)
        BF5 = f5_1
        if (x1 <= 2.6e-005) then f6_1 = -(x1 - (2.6e-005))
          if (2.6e-005 < x1 < 2.8e-005) then begin
p6_1 = (3*(2.6e-005) - 2*(2.6e-005) - (2.8e-005)) / ((2.6e-005) - (2.8e-005))^2
r6_1 = ((2.6e-005) + (2.8e-005) - 2*(2.6e-005)) / ((2.6e-005) - (2.8e-005))^3
f6_1 = p6_1*(x1-(2.8e-005))^2 + r6_1*(x1-(2.8e-005))^3
          end
          if (x1 >= (2.8e-005)) then f6_1 = 0
            BF6 = f6_1
            if (x1 <= 2.2e-005) then f7_1 = 0
              if (2.2e-005 < x1 < 2.6e-005) then begin
p7_1 = (2*(2.6e-005) + (2.2e-005) - 3*(2.5e-005)) / ((2.6e-005) - (2.2e-005))^2
r7_1 = (2*(2.5e-005) - (2.6e-005) - (2.2e-005)) / ((2.6e-005) - (2.2e-005))^3
f7_1 = p7_1*(x1-(2.2e-005))^2 + r7_1*(x1-(2.2e-005))^3
              end
              if (x1 >= (2.6e-005)) then f7_1 = x1 - (2.5e-005)
                BF7 = f7_1
                if (x1 <= 9.5e-006) then f8_1 = 0
                  if (9.5e-006 < x1 < 1.5e-005) then begin
p8_1 = (2*(1.5e-005) + (9.5e-006) - 3*(1e-005)) / ((1.5e-005) - (9.5e-006))^2
r8_1 = (2*(1e-005) - (1.5e-005) - (9.5e-006)) / ((1.5e-005) - (9.5e-006))^3
f8_1 = p8_1*(x1-(9.5e-006))^2 + r8_1*(x1-(9.5e-006))^3
                  end
                  if (x1 >= (1.5e-005)) then f8_1 = x1 - (1e-005)
                    BF8 = f8_1
                    if (x1 <= 4.5e-006) then f9_1 = 0
                      if (4.5e-006 < x1 < 9.5e-006) then begin
p9_1 = (2*(9.5e-006) + (4.5e-006) - 3*(9e-006)) / ((9.5e-006) - (4.5e-006))^2
r9_1 = (2*(9e-006) - (9.5e-006) - (4.5e-006)) / ((9.5e-006) - (4.5e-006))^3
f9_1 = p9_1*(x1-(4.5e-006))^2 + r9_1*(x1-(4.5e-006))^3
                      end
                      if (x1 >= (9.5e-006)) then f9_1 = x1 - (9e-006)
                        BF9 = f9_1
                        if (x1 <= 4.5e-006) then f10_1 = -(x1 - (9e-006))

```

Table 7 Continued

$$\begin{aligned}
 & \text{if } (4.5e-006 < x1 < 9.5e-006) \text{ then begin} \\
 p10_1 &= (3*(9e-006) - 2*(4.5e-006) - (9.5e-006)) / ((4.5e-006) - (9.5e-006))^2 \\
 r10_1 &= ((4.5e-006) + (9.5e-006) - 2*(9e-006)) / ((4.5e-006) - (9.5e-006))^3 \\
 f10_1 &= p10_1*(x1-(9.5e-006))^2 + r10_1*(x1-(9.5e-006))^3 \\
 & \text{end} \\
 & \text{if } (x1 \geq (9.5e-006)) \text{ then } f10_1 = 0 \\
 & \text{BF10} = f10_1 \\
 y &= -2.8 + 1.8e+003*BF1 - 2.7e+003*BF2 - 3.8e+003*BF3 + 1.9e+004*BF4 - 4e+004*BF5 + 2.2e+005*BF6 - \\
 & 1.7e+005*BF7 - 8.4e+004*BF8 + 3.7e+005*BF9 - 3.2e+005*BF10
 \end{aligned}$$

*In this table, x1, x2, x3, and x4 indicate the displacement, damper thickness, diameter, and plate thickness inputs, respectively.

4. Conclusions

In this study, the strength of rotary brace damper was predicted with the use of the usual MLR method and progressive machine-learning methods of MARS. The analogy of MLR and MARS models indicated that the performance of MARS model is better compared to MLR models in predicting RBD strength. The effects of displacement, damper thickness, damper diameter, and plate thickness on damper strength were also investigated. Displacement was found to be the most effective parameter on RBD strength while the plate thickness had no effect. The results indicated that the RBD strength was successfully predicted by MARS using displacement, damper thickness, and diameter inputs. The MARS model increased RMSE and MAE accuracies of the MLR model by 74% and 101%, respectively.

Acknowledgments

This research was supported by Ministry of Higher Education, Malaysia, FRGS/2/2013/TK02/UKM/02/1, University Malaya Research Grant (UMRG – Project No. RP004A/13AET) and Fundamental Research Grant Scheme, Ministry of Education, Malaysia (FRGS – Project No. FP028/2013A) and Birjand University of Technology..

References

- Abdulrahman, A., Ismail, M. and Hussain, M.S. (2011), "Inhibition of corrosion of mild steel in hydrochloric acid by Bambusa arundinacea", *Int. Rev. Mech. Eng.*, **5**(1), 59-63.
- Alhajri, T., Tahir, M., Azimi, M., Mirza, J., Lawan, M., Alenezi, K. and Ragaee, M. (2016), "Behavior of pre-cast U-shaped composite beam integrating cold-formed steel with ferro-cement slab", *Thin Wall Struct.*, **102**, 18-29.
- Ataei, A., Bradford, M.A. and Valipour, H.R. (2015), "Experimental study of flush end plate beam-to-CFST column composite joints with deconstructable bolted shear connectors", *Eng. Struct.*, **99**, 616-630.
- Azimi, M., Adnan, A.B., Osman, M.H., Sam, A.R.B.M., Faridmehr, I. and Hodjati, R. (2014), "Energy absorption capacity of reinforced concrete beam-column connections, with ductility classes low", *Am. J. Civil Eng. Arch.*, **2**(1), 42-52.

- Azimi, M., Adnan, A.B., Tahir, M.M., Sam, A.R.B.M. and Razak, S.M.B.S.A. (2015), "Seismic performance of ductility classes medium RC beam-column connections with continuous rectangular spiral transverse reinforcements", *Lat. Am. J. Solid. Struct.*, **12**(4), 787-807.
- Azimi, M., Ponraj, M., Bagherpourhamedani, A., Tahir, M.M., Razak, S.M.S.A. and Pheng, O.P. (2015), "Shear capacity evaluation of reinforced concrete beams: finite element simulation", *J. Teknologi*, **77**(16).
- Chan, R. and Wong, P. (2014), "A passive rotary system for seismic risk mitigation of steel structures", *Australasian Journal of Construction Economics and Building-Conference Series*.
- Daie, M., Jalali, A., Suhatri, M., Shariati, M., Arabnejad Khanouki, M.M., Shariati, A. and Kazemi Arbat, P. (2011), "A new finite element investigation on pre-bent steel strips as damper for vibration control", *Int. J. Phys. Sci.*, **6**(36), 8044-8050.
- Els, P.S. and Holman, T.J. (1999), "Semi-active rotary damper for a heavy off-road wheeled vehicle", *J. Terramech.*, **36**(1), 51-60.
- Faridmehr, I., Osman, M.H., Tahir, M.M., Nejad, A.F. and Azimi, M. (2015), "Seismic and progressive collapse assessment of new proposed steel connection", *Adv. Struct. Eng.*, **18**(3), 439-452.
- Faris, W.F., Khalid, A.A., Albagul, A. and Ismail, G.A. (2012), "Investigation of the performance of a rotor-bearing system containing composite and non-composite squeeze film dampers", *Mater. Des.*, **34**, 340-345.
- Friedman, J. H. (1991), "Multivariate adaptive regression splines", *Ann. Statist.*, 1-67.
- Hafizah, N., Bhutta, M., Jamaludin, M., Warid, M., Ismail, M., Rahman, M., Yunus, I. and Azman, M. (2014), "Kenaf fiber reinforced polymer composites for strengthening RC Beams", *J. Adv. Concrete Tech.*, **12**(6), 167-177.
- Heysami, A. (2015), "Types of dampers and their seismic performance during an earthquake", *Curr. World Environ.*, **10**, 1002-1015.
- Hibbitt, K., Karlsson, B. and Sorensen, P. (1988), ABAQUS: User's Manual, Hibbitt, Karlsson & Sorensen.
- Huang, L.J., Sheen, Y.N. and Le, D.H. (2014), "On the multiple linear regression and artificial neural networks for strength prediction of soil-based controlled low-strength material", *Applied Mechanics and Materials*, Trans Tech Publication.
- Huang, Q., Xu, Y. and Liu, H. (2015), "An efficient algorithm for simultaneous identification of time-varying structural parameters and unknown excitations of a building structure", *Eng. Struct.*, **98**, 29-37.
- Imaduddin, F., Mazlan, S.A. and Zamzuri, H. (2013), "A design and modelling review of rotary magnetorheological damper", *Mater. Des.*, **51**, 575-591.
- Jalali, A., Daie, M., Nazhadan, S.V.M., Kazemi-Arbat, P. and Shariati, M. (2012), "Seismic performance of structures with pre-bent strips as a damper", *Int. J. Phys. Sci.*, **7**(26), 4061-4072.
- Kang, J.D. and Tagawa, H. (2013), "Seismic response of steel structures with seesaw systems using viscoelastic dampers", *Earthq. Eng. Struct. Dyn.*, **42**(5), 779-794.
- Kawamoto, M., Yamaguchi, K. and Tokahashi, N. (1993), *Rotary damper with improved connection between cap and housing*, Google Patents.
- Khorramian, K., Maleki, S., Shariati, M. and Ramli Sulong, N.H. (2015), "Behavior of Tilted Angle Shear Connectors", *PLoS ONE*, **10**(12), e0144288.
- Mansouri, I. and Kisi, O. (2015), "Prediction of debonding strength for masonry elements retrofitted with FRP composites using neuro fuzzy and neural network approaches", *Compos. Part B: Eng.*, **70**, 247-255.
- McGann, C.R., Bradley, B.A., Taylor, M.L., Wotherspoon, L.M. and Cubrinovski, M. (2015), "Development of an empirical correlation for predicting shear wave velocity of Christchurch soils from cone penetration test data", *Soil Dyn. Earthq. Eng.*, **75**, 66-75.
- Moghaddam, T.B., Soltani, M., Karim, M.R., Shamshirband, S., Petković, D. and Baaj, H. (2015), "Estimation of the rutting performance of Polyethylene Terephthalate modified asphalt mixtures by adaptive neuro-fuzzy methodology", *Constr. Build. Mater.*, **96**, 550-555.
- Moghaddam, T.B., Soltani, M., Shahraki, H.S., Shamshirband, S., Noor, N.B.M. and Karim, M.R. (2016), "The use of SVM-FFA in estimating fatigue life of polyethylene terephthalate modified asphalt mixtures", *Measur.*, **90**, 526-533.
- Mohammadhassani, M., Nezamabadi-Pour, H., Jumaat, M., Jameel, M., Hakim, S. and Zargar, M. (2013),

- “Application of the ANFIS model in deflection prediction of concrete deep beam”, *Struct. Eng. Mech.*, **45**(3), 319-332.
- Mohammadhassani, M., Nezamabadi-Pour, H., Suhatriil, M. and Shariati, M. (2013), “Identification of a suitable ANN architecture in predicting strain in tie section of concrete deep beams”, *Struct. Eng. Mech.*, **46**(6), 853-868.
- Mohammadhassani, M., Suhatriil, M., Shariati, M. and Ghanbari, F. (2014), “Ductility and strength assessment of HSC beams with varying of tensile reinforcement ratios”, *Struct. Eng. Mech.*, **48**(6), 833-848.
- Muhammad, B. and Ismail, M. (2012), “Performance of natural rubber latex modified concrete in acidic and sulfated environments”, *Constr. Build. Mater.*, **31**, 129-134.
- Muhammad, B., Ismail, M., Bhutta, M.A.R. and Abdul-Majid, Z. (2012), “Influence of non-hydrocarbon substances on the compressive strength of natural rubber latex-modified concrete”, *Constr. Build. Mater.*, **27**(1), 241-246.
- Muhammad, N.Z., Keyvanfar, A., Majid, M.Z.A., Shafaghat, A. and Mirza, J. (2015), “Waterproof performance of concrete: A critical review on implemented approaches”, *Constr. Build. Mater.*, **101**, 80-90.
- Muhammad, N.Z., Shafaghat, A., Keyvanfar, A., Majid, M.Z.A., Ghoshal, S., Yasouj, S.E.M., Ganiyu, A.A., Kouchaksaraei, M.S., Kamyab, H. and Taheri, M.M. (2016), “Tests and methods of evaluating the self-healing efficiency of concrete: A review”, *Constr. Build. Mater.*, **112**, 1123-1132.
- Noresson, V., Ohlson, N.G. and Nilsson, M. (2002), “Design of electrorheological dampers by means of finite element analysis: theory and applications”, *Mater. Des.*, **23**(4), 361-369.
- Pranoto, T. and Nagaya, K. (2005), “Development on 2DOF-type and Rotary-type shock absorber damper using MRF and their efficiencies”, *J. Mater. Pr. Tech.*, **161**(1-2), 146-150.
- Salazar, F., Toledo, M., Oñate, E. and Morán, R. (2015), “An empirical comparison of machine learning techniques for dam behaviour modelling”, *Struct. Saf.*, **56**, 9-17.
- Samui, P. and Kim, D. (2013), “Least square support vector machine and multivariate adaptive regression spline for modeling lateral load capacity of piles”, *Neural Comput. Appl.*, **23**(3-4), 1123-1127.
- Scholl, R.E. (1984), “Brace dampers: an alternative structural system for improving the earthquake performance of buildings”, *Proceedings of 8th World Conference on Earthquake Engineering*, San Francisco.
- Schumacher, T. and Shariati, A. (2013), “Monitoring of structures and mechanical systems using virtual visual sensors for video analysis: Fundamental concept and proof of feasibility”, *Sens.*, **13**(12), 16551-16564.
- Shariati, A. and Schumacher, T. (2015), “Oversampling in virtual visual sensors as a means to recover higher modes of vibration”, *41st Annual Review of Progress in Quantitative Nondestructive Evaluation*, **34**, AIP Publishing.
- Shariati, A., Schumacher, T. and Ramanna, N. (2015), “Eulerian-based virtual visual sensors to detect natural frequencies of structures”, *J. Civil Struct. Hlth. Monit.*, **5**(4), 457-468.
- Shariati, M., Ramli Sulong, N.H. and Arabnejad Khanouki, M.M. (2010), “Experimental and analytical study on channel shear connectors in light weight aggregate concrete”, *Proceedings of the 4th International Conference on Steel & Composite Structures*, Sydney, Australia, July.
- Shariati, M., Ramli Sulong, N.H., Arabnejad Khanouki, M.M. and Mahoutian, M. (2011), “Shear resistance of channel shear connectors in plain, reinforced and lightweight concrete”, *Sci. Res. Essay.*, **6**(4), 977-983.
- Shariati, M., Ramli Sulong, N.H., Shariati, A. and Khanouki, M.A. (2015), “Behavior of V-shaped angle shear connectors: experimental and parametric study”, *Mater. Struct.*, **49**(9), 1-18.
- Shariati, M., Ramli Sulong, N.H., Sinaei, H., Arabnejad Khanouki, M.M. and Shafigh, P. (2011), “Behavior of channel shear connectors in normal and light weight aggregate concrete (experimental and analytical study)”, *Adv. Mater. Res.*, **168**, 2303-2307.
- Shariati, M., Sulong, N.R., Suhatriil, M., Shariati, A., Khanouki, M.A. and Sinaei, H. (2012), “Behaviour of C-shaped angle shear connectors under monotonic and fully reversed cyclic loading: An experimental study”, *Mater. Des.*, **41**, 67-73.

- Silva, A., Neves, R. and de Brito, J. (2014), "Statistical modelling of carbonation in reinforced concrete", *Cement Concrete Compos.*, **50**, 73-81.
- Sinaei, H., Shariati, M., Abna, A., Aghaei, M. and Shariati, A. (2012), "Evaluation of reinforced concrete beam behaviour using finite element analysis by ABAQUS", *Sci. Res. Essay.*, **7**(21), 2002-2009.
- Soltani, M., Moghaddam, T.B., Karim, M.R. and Baaj, H. (2015), "Analysis of fatigue properties of unmodified and polyethylene terephthalate modified asphalt mixtures using response surface methodology", *Eng. Fail. Anal.*, **58**, 238-248.
- Symans, M., Charney, F., Whittaker, A., Constantinou, M., Kircher, C., Johnson, M. and McNamara, R. (2008), "Energy dissipation systems for seismic applications: current practice and recent developments", *J. Struct. Eng.*, **134**(1), 3-21.
- Tahmasbi, F., Maleki, S., Shariati, M., Sulong, N.R. and Tahir, M. (2016), "Shear capacity of C-shaped and L-shaped angle shear connectors", *PloS one*, **11**(8), e0156989.
- Umemura, H. (1994), *Rotary oil damper*, Google Patents.
- Yazid, I.I.M., Mazlan, S.A., Kikuchi, T., Zamzuri, H. and Imaduddin, F. (2014), "Design of magnetorheological damper with a combination of shear and squeeze modes", *Mater. Des.*, **54**, 87-95.
- Zhang, W. and Goh, A.T.C. (2013), "Multivariate adaptive regression splines for analysis of geotechnical engineering systems", *Comput. Geotech.*, **48**, 82-95.